Magnetoplasmon-phonon coupling in semiconductor quantum wells

1990 J. Phys.: Condens. Matter 2 8881

(http://iopscience.iop.org/0953-8984/2/45/004)

J. Phys.: Condens. Matter **2** (1990) 8881–8904. Printed in the UK

Magnetoplasmon–phonon coupling in semiconductor quantum wells

L Wendler and R Pechstedt†

Sektion Physik der Friedrich-Schiller-Universität Jena, Max-Wien-Platz 1, Jena, DDR-6900, German Democratic Republic

Received 7 August 1989, in final form 21 May 1990

Abstract. The collective excitations of a double heterostructure in the presence of a magnetic field are examined in detail. The polarization function of the quasi-two-dimensional electron gas in the presence of a perpendicular quantizing magnetic field is calculated within various long-wave approximations and in the random-phase approximation. Using these polarization functions the dispersion curves of the coupled intra- and inter-subband magnetoplasmon–phonons are calculated and plotted in graphical form. The calculation of the dispersion relation is done for GaAs–$Ga_{1-x}Al_xAs$ double heterostructures and include both quantum size effects and the correct spectrum of the long-wave optical phonons. In this paper the higher resonances of the quasi-two-dimensional magnetoplasma, the Bernstein modes, are also investigated. It is shown that the intra- and inter-subband magnetoplasmon–phonons are free of Landau damping for finite perpendicular quantizing magnetic fields.

1. Introduction

In recent years there has been a great deal of interest on collective excitations in semiconductor microstructures such as heterostructures, quantum wells and superlattices. It is possible to produce these systems, which are typified by heterointerfaces between the different semiconductors, due to the recent advent of novel epitaxial growth techniques. In modulation-doped systems the electrons form a gas with a dimension between two and three. In simple quantum wells the electron motion is quasi-free parallel to the heterointerfaces, but confined within a narrow channel by a one-dimensional potential. Because the width of this channel is usually of the order of the de Broglie wavelength of the electrons, and at low temperatures is much smaller than the elastic mean free path of the electrons, they form a quasi-two-dimensional electron gas (Q2DEG), i.e. the spectrum of the electrons consists of discrete subbands. This is true because the subband spacing is much larger than the energy broadening induced by scattering processes.

If a magnetic field is applied perpendicular to the heterointerfaces, the motion of the electrons of the Q2DEG is completely quantized. The discreteness of the eigenvalue spectrum is essential for the occurrence of the quantum Hall effect. Further, this complete quantized situation for the electrons of the Q2DEG results in novel properties

† Present address: Akademie der Wissenschaften der DDR, Zentralinstitut für Physik der Erde, Burgweg 11, Jena, DDR-6900, German Democratic Republic.

0953-8984/90/458881 + 24 $03.50

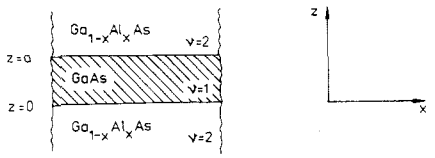

Figure 1. Schematic diagram of the geometry of a double heterostructure.

of the collective excitations, for example the quantized undamping of helicon waves (Wendler and Kaganov 1986a, b, 1987).

It is well known that the electron gas can support charge-density oscillations, plasmons, organized by long-range Coulomb fields. In the presence of a magnetic field the corresponding collective excitations are magnetoplasmons. Magnetoplasmons have been of considerable interest in the past few years. For a strict 2DEG magnetoplasmons were investigated theoretically by Chaplik (1972) within a local approximation. Chiu and Quinn (1974) considered the effect of retardation on the modes and Horing and Yildiz (1976) and Glasser (1983) calculated the polarization function of the 2D magnetoplasma within the random-phase approximation. More recently 2D magnetoplasmons and magnetic excitons have been studied in the Hartree–Fock approximation (Lerner and Lozovik 1978, Bychkov *et al* 1981, Kallin and Halperin 1984, MacDonald 1985). The previous studies have been restricted to integral filling factors of the Landau levels, whereas the case of non-integral filling factors was investigated by Oji and MacDonald (1986a). Magnetoplasmons are also investigated in detail for superlattices (Kobayashi *et al* 1975, Das Sarma and Quinn 1982, Bloss and Brody 1982, Tselis and Quinn 1984a, b, Gasser and Täuber 1987). Horing and Yildiz (1986) analysed in RPA the dynamic non-local longitudinal dielectric response of a magnetoplasma confined within a layer of finite thickness. But the results obtained were on a semi-classical level, because the boundary condition of specular reflection was used for the electrons (classical infinite barrier model). Q2D magnetoplasmons were investigated experimentally by far-infrared spectroscopy on Si–MOS systems (Theis *et al* 1977, Mohr and Heitmann 1982) and on GaAs–$Ga_{1-x}Al_xAs$ heterostructures (Batke *et al* 1985, 1986).

Most of the semiconductor microstructures are made from the weakly polar compound semiconductor materials of the III–V series. In polar semiconductors long-wave optical lattice vibrations are accompanied by macroscopic electric fields and hence, they couple to the electrons of the Q2DEG. This is the Fröhlich type of electron–phonon interaction which leads to a strong coupling between the magnetoplasmons and the long-wave optical phonons, if their frequencies are comparable. Magnetoplasmon–phonon coupling is investigated by Tselis and Quinn (1984b) for a superlattice, using a long-wavelength approximation of the polarization function, and by Oji and MacDonald (1986b), using the RPA polarization function. In these works only the coupling to the ordinary bulk 3D longitudinal-optical (LO) phonons is treated. But a real semiconductor microstructure is a layered system and hence the spectrum of the optical phonons interacting with the electrons is altered by the interfaces of the system (Wendler 1985). The ordinary dispersion-free LO phonons are changed to be modes confined in each individual layer, having electric fields with vanishing influence at the interfaces, implying that 3D wavevectors smaller than $|q| = \pi/a$ (where a is the layer thickness) are forbidden. And further, new states, interface phonons, occur in the spectrum of the optical phonons with fields mainly localized at the interfaces of the system and decaying exponentially from them.

In recent papers (Wendler and Pechstedt 1986, 1987a, b, Wendler 1988, Wendler *et al* 1988, 1990, Wendler and Grigoryan 1989) we have studied the plasmon–phonon coupling in heterostructures and quantum wells. The emphasis of this paper is to generalize our previous work to the case of an applied homogeneous magnetic field. We represent a RPA calculation of coupled magnetoplasmon–phonons in double heterostructures including both quantum size effects and the correct spectrum of the long-wave optical phonons. We also investigate the higher resonances of the Q2D magnetoplasma, the Bernstein modes, and their interaction with both the principal magnetoplasmons and the optical phonons.

2. Electronic subband structure

The DHS (figure 1) which is under consideration in the present paper consists of a smaller-gap semiconductor ($\nu = 1$) for $a > z > 0$ (for instance GaAs), which is symmetrically embedded between a wider-gap semiconductor ($\nu = 2$) for $z > a$ and $0 > z$ (for instance $Ga_{1-x}Al_xAs$).

The single-particle Hamiltonian in effective-mass approximation for the electrons of the Q2DEG in the presence of a quantizing homogeneous DC magnetic field $\boldsymbol{B} = (0, 0, B)$, applied perpendicularly to the heterointerfaces is given by

$$H_0 = \frac{1}{2m}\left(\frac{\hbar}{\mathrm{i}}\boldsymbol{\nabla} + e\boldsymbol{A}\right)^2 + V_{\mathrm{eff}}(z) + \frac{g^*}{2}\mu_{\mathrm{B}}B\sigma_z. \tag{1}$$

Here, $\boldsymbol{A}$ is the vector potential with $\boldsymbol{B} = \boldsymbol{\nabla} \times \boldsymbol{A}$ and $V_{\mathrm{eff}}(z)$ is the effective confining potential resulting from the conduction-band offset at the heterointerfaces and from the charges in the system. $\mu_{\mathrm{B}} = e\hbar/(2m_0)$ denotes Bohr's magneton, m_0 the free electron mass in contrast to the effective electron mass m, g^* the effective spin-splitting (Landé) factor and σ_z denotes the Pauli matrix. With the use of the Landau gauge $\boldsymbol{A} = (0, xB, 0)$ the eigenvalue problem of the Hamiltonian (1) becomes equivalent to two separate equations, one for the size quantization and one for the magnetic quantization. According to the symmetry properties of the system the single-particle wavefunction is

$$\langle \boldsymbol{x}|KNk_y\sigma\rangle = \psi_{KNk_y\sigma}(\boldsymbol{x}) = (1/\sqrt{L_y})\,\mathrm{e}^{\mathrm{i}k_y y}\phi_N(x + k_y l_0^2)\varphi_K(z)\chi_\sigma \tag{2}$$

and for the one-electron energy follows with (1) and (2):

$$\varepsilon_{KN\sigma} = \varepsilon_K + \varepsilon_N + g^*\mu_{\mathrm{B}}B\sigma \tag{3}$$

where $l_0 = (\hbar/eB)^{1/2}$ is the magnetic length, χ_σ are the two spin eigenfunctions for spin-up and spin-down along the z axis and σ takes the values $+\frac{1}{2}$ and $-\frac{1}{2}$. We have applied Born–von Kárman periodic boundary conditions in the y direction with unit length L_y.

The effective potential $V_{\mathrm{eff}}(z)$ affects the electron motion in z direction. It causes their spatial confinement within a narrow channel, which has a width of the same order as the de Broglie wavelength of the electrons. This leads to a sequence of subbands (size quantization). The subband energies ε_K are determined by solving the one-dimensional Schrödinger equation for the envelope wavefunction $\varphi_K(z)$ of an electron in the Kth subband. This Schrödinger equation follows from equations (1)–(3) and reads:

$$\left(-\frac{\hbar^2}{2m}\frac{\mathrm{d}^2}{\mathrm{d}z^2} + V_{\mathrm{eff}}(z)\right)\varphi_K(z) = \varepsilon_K\varphi_K(z). \tag{4}$$

For the analytic and numerical calculations in the following sections we are interested in

the simplest model potential neglecting band-bending and exchange-correlation effects due to the charges in the system, and infinite barriers are assumed for the quantum well:

$$V_{\text{eff}}(z) = \begin{cases} 0; & a > z > 0 \\ \infty; & \text{otherwise.} \end{cases} \tag{5}$$

Within this simple infinite square well potential model the normalized envelope wavefunction is given by

$$\varphi_K(z) = \sqrt{\frac{2}{a}} - \sin\left(\frac{\pi(K+1)}{a} z\right) \qquad K = 0, 1, 2, \ldots \tag{6}$$

and the subband energies are

$$\varepsilon_K = \frac{\hbar^2 \pi^2}{2ma^2} (K+1)^2. \tag{7}$$

The magnetic field applied in the z direction affects the electron motion in the x–y plane (magnetic quantization). Hence, using the above-mentioned Landau gauge the eigenvalue problem is that of a one-dimensional harmonic oscillator with a displaced centre $X = -l_0^2 k_y$. Then the corresponding eigenfunctions are:

$$\phi_N(x + l_0^2 k_y) = [1/(2^N N! \pi^{1/2} l_0)^{1/2}] \exp[-(1/2l_0^2)(x + l_0^2 k_y)^2] H_N(1/l_0)(x + l_0^2 k_y) \tag{8}$$

and the eigenvalues are given by

$$\varepsilon_N = \hbar\omega_c (N + \tfrac{1}{2}) \qquad N = 0, 1, 2, \ldots \tag{9}$$

where $\omega_c = eB/m$ is the cyclotron frequency and $H_N(\xi)$ is the Hermite polynomial.

Since the energy eigenvalues $\varepsilon_{KN\sigma}$ are independent of the quantum number k_y each energy level is degenerate. For a finite system the allowed values of the quantum number k_y are separated by $2\pi/L_y$ so that the total number N_L of k_y values belonging to the same energy $\varepsilon_{KN\sigma}$ is:

$$N_L = (eB/h)A \qquad A = L_x L_y. \tag{10}$$

The degeneracy factor is identical to the number of flux quanta ($\phi_0 = h/e$: magnetic flux quantum) within the area A. The manifold states associated with the quantum numbers $\{N\sigma\}$ are referred to as Landau levels. Thus, the quantum number k_y (or the centre coordinate X) labels all the states within one Landau level.

The application of this quantum description to real 2D electronic systems is limited by the appearance of scattering processes. Scattering processes result in a broadening of the Landau levels. Hence, the quantum description is valid if this energy broadening, $\Delta E \sim \hbar/\tau$ (τ is the collision time of the electrons), is much smaller than the spacing $\hbar\omega_c$ between the Landau levels. Further, we note that in microstructures composed of III–V semiconductors and magnetic fields in the order of 2–5 T the radius of the cyclotron motion is comparable to the de Broglie wavelength and it is small in comparison with the mean free path $l = v_F \tau$ ($\simeq$1000 nm for a typical semiconductor; $v_F = \hbar k_F/m$ is the Fermi velocity; $k_F = (2\pi n_{2DEG})^{1/2}$ the 2D Fermi wavevector) of the electrons. Following this we assume in this paper that the magnetic fields are quantizing magnetic fields.

Many of the unusual properties of the discussed system are due to two important facts. One is that Landau levels have a macroscopic degeneracy associated with the

centre coordinate of the cyclotron motion. The other is connected with the fact that we have a completely quantized situation in the Q2DEG in the presence of a perpendicular magnetic field, since there is no continuum of extended states associated with kinetic energy motion parallel to the magnetic field, so there is no continuum aspect to the spectrum of uncorrelated electron states. Such an energy spectrum consisting of energy levels separated by gaps is essential for the quantum Hall effect.

3. The polarization function of the Q2D magnetoplasma

3.1. The dynamically screened potential

The electrons of the Q2DEG can be scattered in two ways, by electron–electron interaction and, since the Q2DEG is embedded within a polar semiconductor, by electron–phonon interaction. In the first case the scattering process is mediated by the bare (or direct) Coulomb interaction, while in the second case the electrons interact by sending a long-wave phonon from one electron to the other. Since the Q2DEG is polarizable, this interaction is screened and the bare interaction potential $W(\boldsymbol{x}, \boldsymbol{x}' \,|\, \omega)$, which is the sum of the above mentioned two contributions, must be replaced by the screened interaction potential $W^{\mathrm{sc}}(\boldsymbol{x}, \boldsymbol{x}' \,|\, \omega)$ between the electrons. This screened interaction potential obeys the integral equation (Mahan 1972a)

$$W^{\mathrm{sc}}(\boldsymbol{x}, \boldsymbol{x}' \,|\, \omega) = W(\boldsymbol{x}, \boldsymbol{x}' \,|\, \omega) + \int \mathrm{d}^3 x'' \int \mathrm{d}^3 x''' \, W(\boldsymbol{x}, \boldsymbol{x}'' \,|\, \omega) \, P^H(\boldsymbol{x}'', \boldsymbol{x}''' \,|\, \omega) \times W^{\mathrm{sc}}(\boldsymbol{x}''', \boldsymbol{x}' \,|\, \omega) \tag{11}$$

where $P^H(\boldsymbol{x}, \boldsymbol{x}' \,|\, \omega)$ is the proper polarization function of the Q2D magnetoplasma in the presence of a perpendicular magnetic field. The dynamically screened interaction potential contains all information necessary in order to describe the collective excitations of this system.

At first, however, we discuss the properties of the polarization function. In general, the polarization function contains both internal Coulomb and phonon lines. In this paper we are concerned with the random-phase approximation of the polarization function $P^H(\boldsymbol{x}, \boldsymbol{x}' \,|\, \omega)$, which is given by the single-loop approximation:

$$P^H(\boldsymbol{x}, \boldsymbol{x}' \,|\, \mathrm{i}\omega_n) = \frac{2}{\beta} \sum_{\mathrm{i}\nu_n} \mathcal{G}^{(0)}(\boldsymbol{x}, \boldsymbol{x}' \,|\, \mathrm{i}\nu^n + \mathrm{i}\omega_n) \, \mathcal{G}^{(0)}(\boldsymbol{x}', \boldsymbol{x} \,|\, \mathrm{i}\nu_n) \tag{12}$$

with $\mathcal{G}^{(0)}(\boldsymbol{x}, \boldsymbol{x}' \,|\, \mathrm{i}\nu_n)$ the unperturbed single-particle temperature Green's function of an electron. This Green's function is given by

$$\mathcal{G}^{(0)}(\boldsymbol{x}, \boldsymbol{x}' \,|\, \mathrm{i}\nu_n) = \frac{1}{L_y} \sum_{KNk_y} \frac{\exp[\mathrm{i}k_y(y-y')] \phi_N(x + k_y l_0^2) \phi_N^*(x' + k_y l_0^2)}{\mathrm{i}\hbar\nu_n - \xi_{KN}} \varphi_K(z) \varphi_K^*(z'). \tag{13}$$

Here, $\nu_n = (2n+1)\pi/\beta\hbar$ and $\omega_n = (2n)\pi/\beta\hbar$ are Matsubara frequencies, where n is an integral number, $\beta = 1/k_{\mathrm{B}}T$ and $\xi_{KN} = \varepsilon_{KN} - \mu$ with μ the chemical potential. The retarded polarization function is obtained by the usual analytic continuation $\mathrm{i}\omega_n \rightarrow \omega + \mathrm{i}\delta$, $\delta \rightarrow 0^+$. For simplicity we have assumed the spin-splitting factor g^* to be zero but the spin degeneracy is included. This is a reasonable approximation because in the case of GaAs the spin-splitting is at least five times smaller than the Landau level

separation even if many-electron enhancement of the g^*-factor is included (Nicholas *et al* 1988).

By performing the summation over the Matsubara frequencies one derives

$$P^H(\boldsymbol{x}_\parallel - \boldsymbol{x}'_\parallel; z, z' | i\omega_n) = \frac{1}{A}\sum_{\boldsymbol{q}_\parallel} \exp[i\boldsymbol{q}_\parallel(\boldsymbol{x}_\parallel - \boldsymbol{x}'_\parallel)] P^H(\boldsymbol{q}_\parallel; z, z' | i\omega_n) \tag{14}$$

with

$$P^H(\boldsymbol{q}_\parallel; z, z' | i\omega_n) = \sum_{KK'} \varphi_K(z)\varphi^*_K(z')\varphi_{K'}(z')\varphi^*_{K'}(z) P^H_{KK'}(\boldsymbol{q}_\parallel, i\omega_n) \tag{15}$$

and

$$P^H_{KK'}(\boldsymbol{q}_\parallel, i\omega_n) = \frac{1}{\pi l_0^2}\sum_{NN'} \frac{n_F(\xi_{K'N'}) - n_F(\xi_{KN})}{i\hbar\omega_n + \xi_{K'N'} - \xi_{KN}} |J_{NN'}(\boldsymbol{q}_\parallel)|^2 \tag{16}$$

where $\boldsymbol{x}_\parallel$ and $\boldsymbol{q}_\parallel$ are the two-dimensional position and wavevector in the x–y plane. In equation (16) n_F denotes the Fermi occupancy factor for the electrons and $J_{NN'}(\boldsymbol{q}_\parallel)$ is defined by

$$J_{NN'}(\boldsymbol{q}_\parallel) = \int dx \exp(iq_x x)\phi^*_N(x + q_y l_0^2)\phi_{N'}(x). \tag{17}$$

A straightforward calculation shows that $|J_{NN'}(\boldsymbol{q}_\parallel)|^2$ can be expressed as

$$|J_{NN'}(\boldsymbol{q}_\parallel)|^2 = (N_2!/N_1!)[(l_0^2/2)q_\parallel^2]^{N_1 - N_2} \exp[-(l_0^2/2)q_\parallel^2]\{L_{N_2}^{N_1 - N_2}[(l_0^2/2)q_\parallel^2]\}^2 \tag{18}$$

with $N_1 = \max(N, N')$ and $N_2 = \min(N, N')$. $L_N^{N'}(\xi)$ is the associated Laguerre polynomial. Using (14) to (16) the integral equation (11) can be rewritten to an algebraic one in the 'subband space' (Wendler and Pechstedt 1986)

$$W^{sc}_{K_1K_2K_3K_4}(\boldsymbol{q}_\parallel, \omega) = W_{K_1K_2K_3K_4}(\boldsymbol{q}_\parallel, \omega) + \sum_{LL'} W_{K_1K_2L'L}(\boldsymbol{q}_\parallel, \omega) P^H_{LL'}(\boldsymbol{q}_\parallel, \omega) W^{sc}_{LL'K_3K_4}(\boldsymbol{q}_\parallel, \omega). \tag{19}$$

In this equation the bare interaction potential is given by

$$W_{K_1K_2K_3K_4}(\boldsymbol{q}_\parallel, \omega) = V^\infty_{K_1K_2K_3K_4}(\boldsymbol{q}_\parallel) + V^{ph}_{K_1K_2K_3K_4}(\boldsymbol{q}_\parallel, \omega) \tag{20}$$

where

$$V^{ph}_{K_1K_2K_3K_4}(\boldsymbol{q}_\parallel, \omega) = \frac{2}{\hbar}\sum_j \frac{\omega_j(\boldsymbol{q}_\parallel)}{(\omega + i\delta)^2 - \omega_j^2(\boldsymbol{q}_\parallel)} M^j_{K_1K_2}(\boldsymbol{q}_\parallel) M^j_{K_3K_4}(-\boldsymbol{q}_\parallel) \tag{21}$$

is the phonon-mediated equivalent electron–electron interaction potential and

$$V^\infty_{K_1K_2K_3K_4}(\boldsymbol{q}_\parallel) = \frac{e^2}{2\varepsilon_0\varepsilon_\infty q_\parallel}\int dz \int dz' \, \varphi^*_{K_1}(z)\varphi_{K_2}(z) \exp(-q_\parallel|z - z'|)\varphi^*_{K_3}(z')\varphi_{K_4}(z') \tag{22}$$

describes the bare electron–electron (direct Coulomb) interaction. $\omega_j(\boldsymbol{q}_\parallel)$ is the dispersion relation of the jth long-wave optical phonon mode in the layered structure and the vertex function $M^j_{KK'}(\boldsymbol{q}_\parallel)$ is given by

$$M^j_{KK'}(\boldsymbol{q}_\parallel) = \sqrt{A} \int \mathrm{d}z\, \varphi^*_K(z)\Gamma_j(\boldsymbol{q}_\parallel, z)\varphi_{K'}(z). \tag{23}$$

Here $\Gamma_j(\boldsymbol{q}_\parallel, z)$ is the coupling function (Wendler 1985) describing the coupling strength of a single electron with the jth optical phonon mode of the DHS and it is discussed in detail by Wendler and Pechstedt (1987b) for a DHS and by Wendler *et al* (1990) for a heterostructure.

In equation (22) the bare electron–electron interaction potential is screened by the high-energy electronic excitations across the band gap, represented by the optical dielectric constant of the semiconductor containing the Q2D magnetoplasma. We omit in the bare interaction potential the classical image potential in the electron–electron interaction, which arises by solving Poisson's equation in a layered structure. The reason is that we take into account the phonon-mediated interaction potential, which gives the major contribution to the classical image potential on a quantum mechanical level (Mahan 1972b, Evans and Mills 1973). The remaining terms are mysterious and its neglect is a good approximation because of its very small magnitude.

In the following we take into account the assumption of the electric quantum limit. That means, in equilibrium the electrons only occupy the lowest ($K = 0$) subband. According to this assumption the matrix polarization function $P^H_{KK'}$ has at zero temperature only the non-vanishing elements P^H_{00}, P^H_{0K} and P^H_{K0}. In this case equation (15) can be written in the form:

$$P^H(\boldsymbol{q}_\parallel; z, z'|\omega) = \sum_K \varphi_0(z)\varphi_0(z')\varphi_K(z')\varphi_K(z)\chi^H_K(\boldsymbol{q}_\parallel, \omega) \tag{24}$$

with

$$\chi^H_K(\boldsymbol{q}_\parallel, \omega) = \begin{cases} P^H_{00}(\boldsymbol{q}_\parallel, \omega) & \text{if } K = 0 \\ P^H_{K0}(\boldsymbol{q}_\parallel, \omega) + P^H_{0K}(\boldsymbol{q}_\parallel, \omega) & \text{if } K > 0. \end{cases} \tag{25}$$

The polarization function $\chi^H_K(\boldsymbol{q}_\parallel, \omega)$ contains two physically different contributions:

(i) the intrasubband contribution for $K = 0$ arising from an electron excitation above the Fermi sea within the lowest subband, and

(ii) the intersubband contribution for $K > 0$ arising from an electron excitation to higher subbands.

Within the electric quantum limit it is possible to simplify equation (19) by setting $K_2 = K_4 = 0$ in the interaction potentials, and then using (25) gives

$$W_{KK'}(\boldsymbol{q}_\parallel, \omega) = \sum_L [\delta_{KL} - W_{KL}(\boldsymbol{q}_\parallel, \omega)\chi^H_L(\boldsymbol{q}_\parallel, \omega)]W^{sc}_{LK'}(\boldsymbol{q}_\parallel, \omega). \tag{26}$$

The condition for the existence of collective excitations, the dispersion relation, follows from equation (26) under the condition that $V^c_{KK'} = 0$ while $W^{sc}_{KK'} \neq 0$. $V^c_{KK'}$ corresponds to the potential $V^\infty_{KK'}$ given in (22) with $\varepsilon_\infty = 1$. The resulting dispersion relation has the form:

$$\det[\delta_{KL} - W_{KL}(\boldsymbol{q}_\parallel, \omega)\chi^H_L(\boldsymbol{q}_\parallel, \omega)] = 0. \tag{27}$$

It was shown (Wendler *et al* 1988) that according to the symmetry properties of the DHS

the bare interaction potential has the following properties: $W_{00} \neq 0$, $W_{11} \neq 0$, $W_{10} = W_{01} = 0$, $W_{22} \neq 0$, $W_{20} = W_{02} \neq 0$ and $W_{21} = W_{12} = 0$. Because of the large energetic separation between the 0th and the 2nd subband at the usual layer thicknesses of a DHS the contribution of W_{20} is very weak in magnitude. Therefore it is a very good approximation to neglect the off-diagonal elements in (27). This means that intra- and intersubband modes are decoupled. Within this approximation equation (27) takes the form:

$$W_{KK}^{-1}(\boldsymbol{q}_\parallel, \omega) - \chi_K^H(\boldsymbol{q}_\parallel, \omega) = 0. \tag{28}$$

Since the dispersion relation contains long-wave optical phonons (both interface and LO phonons) as well as charge-density excitations of the Q2D magnetoplasma, it describes:

(i) coupled intrasubband magnetoplasmon–phonon modes if $K = 0$, and
(ii) coupled intersubband magnetoplasmon–phonon modes if $K > 0$.

A very interesting result is obtained if we consider the dispersion relation (28) in the limit $a \to 0$, i.e. a strict 2DEG embedded in the semiconductor $\nu = 2$. In this limit all the electrons occupy only the lowest $K = 0$ subband since the layer is so thin that the energy differences between the different subbands are very large. Further, electron transitions between the lowest and higher subbands cannot take place at low temperatures. In this case the de Broglie wavelength of the electrons is much larger than the layer thickness. Considering this physical situation it is possible to derive the following relations:

$$\lim_{a\to 0} V_{00}^{\infty}(\boldsymbol{q}_\parallel) = e^2/2\varepsilon_0\varepsilon_{\infty 2}q_\parallel \tag{29}$$

where we have replaced $\varepsilon_{\infty 1}$ by $\varepsilon_{\infty 2}$ because for $a \to 0$ the underground dielectric constant is now $\varepsilon_{\infty 2}$, and further

$$\lim_{a\to 0} M_{00}^{\mathrm{L1}}(\boldsymbol{q}_\parallel) = 0 \tag{30}$$

$$M_{00}^{\mathrm{A}\pm}(\boldsymbol{q}_\parallel) = 0 \tag{31}$$

$$\lim_{a\to 0} M_{00}^{\mathrm{S}+}(\boldsymbol{q}_\parallel) = -[e^2\hbar(\omega_{\mathrm{L}2}^2 - \omega_{\mathrm{T}2}^2)/4\varepsilon_0\varepsilon_{\infty 2}\omega_{\mathrm{L}2}q_\parallel]^{1/2} \tag{32}$$

$$\lim_{a\to 0} M_{00}^{\mathrm{S}-}(\boldsymbol{q}_\parallel) = 0. \tag{33}$$

Herein L1, A± and S± denote the different types of long-wave optical phonons, i.e. the LO phonons of the GaAs layer (L1), the antisymmetric (A±) and the symmetric (S±) interface phonons. These vertex functions are explicitly given by Wendler and Pechstedt (1987b). Using these relations for the vertex functions of the optical phonons in the definition of the electron–phonon potential we obtain

$$V_{00}^{\mathrm{ph}}(\boldsymbol{q}_\parallel, \omega) = \frac{e^2\omega_{\mathrm{L}2}^2}{2\varepsilon_0 q_\parallel}\left(\frac{1}{\varepsilon_{\infty 2}} - \frac{1}{\varepsilon_{\mathrm{s}2}}\right)\frac{1}{(\omega + \mathrm{i}\delta)^2 - \omega_{\mathrm{L}2}^2}. \tag{34}$$

Herein $\omega_{\mathrm{L}2}$ and $\omega_{\mathrm{T}2}$ are the longitudinal and transverse (LO and TO) phonon frequencies and $\varepsilon_{\infty 2}$ and $\varepsilon_{\mathrm{s}2}$ are the optical and the static dielectric constant of the semiconductor material forming the barriers of the DHS. Equation (34) represents the electron–phonon interaction potential for the interaction of an electron with 3D bulk LO phonons of medium $\nu = 2$ (Wendler and Pechstedt 1987b). Hence, in the strict 2D limit the electrons only interact with these optical phonons.

If one compares equation (28) with the corresponding equation without magnetic field (Wendler and Pechstedt 1986), it can be seen that the difference between these two cases is only given by the different polarization functions. Hence, for the calculation of the dispersion relation, a detailed knowledge of the polarization function is necessary.

3.2. Intrasubband contribution of the polarization function

According to (25) we found by a little algebra from (16) the retarded polarization function for $K = 0$ in the form:

$$\chi_0^H(\boldsymbol{q}_\parallel, \omega) = \frac{2}{\hbar\pi l_0^2} \sum_{N=0}^{\infty} \sum_{S=1}^{\infty} [n_F(\xi_{0N}) - n_F(\xi_{0N+S})] |J_{N+S,N}(\boldsymbol{q}_\parallel)|^2 \frac{S\omega_c}{(\omega + i\delta)^2 - (S\omega_c)^2}. \tag{35}$$

This polarization function inserted in the dispersion relation (28) describes the coupled intrasubband magnetoplasmon–phonons, where the $S = 1$ term of (35) is the contribution of the principal intrasubband magnetoplasmon. The higher resonances in (35) are the contributions of the intrasubband Bernstein modes which couple with the principal intrasubband magnetoplasmon and with the long-wave optical phonons. The imaginary part of the polarization function is found from (35):

$$\operatorname{Im} \chi_0^H(\boldsymbol{q}_\parallel, \omega) = -\frac{1}{\hbar l_0^2} \sum_{N=0}^{\infty} \sum_{S=1}^{\infty} [n_F(\xi_{0N}) - n_F(\xi_{0N+S})] |J_{N+S,N}(\boldsymbol{q}_\parallel)|^2 \times [\delta(\omega - S\omega_c) - \delta(\omega + S\omega_c)]. \tag{36}$$

This result means that the coupled intrasubband magnetoplasmon–phonons could only be damped at the frequencies $\omega = \pm S\omega_c$. But at these certain frequencies $\operatorname{Re} \chi_0^H(\boldsymbol{q}_\parallel, \omega)$ has poles and therefore no root of the dispersion relation (28) can lie on any multiple of ω_c. Hence, there is no Landau damping of the coupled intrasubband modes for all temperatures within the RPA for finite perpendicular *quantizing* magnetic fields. However, it is important to note that in the zero magnetic field limit the intrasubband Bernstein modes lose their identity as distinct plasmon resonances, and only the intrasubband plasmon remains, which now become Landau damped in the single-particle intrasubband continuum (Wendler 1988).

For further discussion of the properties of intrasubband magnetoplasmon–phonons we restrict our attention to some approximations of the polarization function (35) at $T = 0$ K. At first we consider the long-wave approximation by expanding $|J_{N+S,N}(\boldsymbol{q}_\parallel)|^2$ to $O(q_\parallel^4)$. In this case one has to take only the $S = 1$ and $S = 2$ terms, and carrying out the summation over the Landau levels (N) in (35), one obtains (see appendix)

$$\chi_0^H(\boldsymbol{q}_\parallel, \omega) = \frac{n_{2DEG}}{m} \frac{q_\parallel^2}{\omega^2 - \omega_c^2} - \frac{n_{2DEG}^2 \pi l_0^4}{2m} q_\parallel^4 \left(\frac{1}{\omega^2 - \omega_c^2} - \frac{1}{\omega^2 - (2\omega_c)^2} \right) \tag{37}$$

where n_{2DEG} is the sheet carrier concentration of the Q2DEG (electron concentration per unit area). Within this long-wave approximation it is very simple to show that in the limit $B \to 0$ the intrasubband Bernstein modes lose their identity. From equation (37) it follows:

$$\lim_{B \to 0} \chi_0^H(\boldsymbol{q}_\parallel, \omega) = (n_{2DEG} q_\parallel^2 / m\omega^2)[1 + (\tfrac{3}{4} v_F^2 q_\parallel^2)/\omega^2]. \tag{38}$$

Equation (38) represents the well known result of the intrasubband contribution to the

polarization function without any magnetic field (compare for instance with (67) in Wendler and Pechstedt 1986). Hence, (38) describes only one mode, the intrasubband plasmon.

As a further approximation we consider the polarization function for the case where only the lowest Landau level is filled. In this case the full RPA polarization function for $T = 0$ K is given by the analytic expression:

$$\chi_0^H(\boldsymbol{q}_\parallel, \omega) = \frac{2\omega_c}{\hbar\pi l_0^2} \exp(-l_0^2 q_\parallel^2/2) \sum_{N=1}^{\infty} \frac{(l_0^2 q_\parallel^2/2)^N}{(N-1)!} \frac{1}{\omega^2 - (N\omega_c)^2}. \tag{39}$$

If one includes only the contribution to the polarization function from transitions between the $N = 0$ and the $N = 1, 2$ Landau levels, the full RPA result is given by:

$$\chi_0^H(\boldsymbol{q}_\parallel, \omega) = \frac{\omega_c}{\hbar\pi} \exp(-l_0^2 q_\parallel^2/2) \left(\frac{q_\parallel^2}{(\omega + i\delta)^2 - \omega_c^2} + \frac{l_0^2 q_\parallel^4/2}{(\omega + i\delta)^2 - (2\omega_c)^2} \right). \tag{40}$$

Without the last term in the brackets this polarization function is discussed by Oji and MacDonald (1986b), because they include only the contribution from transitions between the $N = 0$ and the $N = 1$ Landau levels. By expanding the exponential function in (40) and using the fact that only the lowest Landau level is filled ($\omega_c/\hbar\pi = n_{2DEG}/m$) one of course recovers (37).

3.3. Intersubband contribution of the polarization function

For the intersubband contribution of the polarization function we found for $K > 0$ from (16) and (25):

$$\chi_K^H(\boldsymbol{q}_\parallel, \omega) = \frac{2}{\hbar\pi l_0^2} \sum_{N=0}^{\infty} \left(\sum_{S=0}^{\infty} n_F(\xi_{0N}) |J_{N+S,N}(\boldsymbol{q}_\parallel)|^2 \frac{\Omega_{K0} + S\omega_c}{(\omega + i\delta)^2 - (\Omega_{K0} + S\omega_c)^2} \right.$$
$$\left. + \sum_{S=1}^{\infty} n_F(\xi_{0N+S}) |J_{N+S,N}(\boldsymbol{q}_\parallel)|^2 \frac{\Omega_{K0} - S\omega_c}{(\omega + i\delta)^2 - (\Omega_{K0} - S\omega_c)^2} \right) \tag{41}$$

where we have used the condition of the electric quantum limit by $n_F(\xi_{KN}) = 0$ for $K > 0$.

In equation (41) $\Omega_{K0} = (\varepsilon_K - \varepsilon_0)/\hbar$ is the subband separation frequency. The polarization function (41) inserted in the dispersion relation (28) describes the coupled intersubband magnetoplasmon–phonons. The term of (41) with $S = 0$ is the contribution of the principal intersubband magnetoplasmon and the higher resonances ($S > 0$) are the contributions of the intersubband Bernstein modes which couple with both the principal intersubband magnetoplasmon as well as with the long-wave optical phonons. The imaginary part of the polarization function is found from (41):

$$\operatorname{Im} \chi_K^H(\boldsymbol{q}_\parallel, \omega) = -\frac{1}{\hbar l_0^2} \sum_{N=0}^{\infty} \left(\sum_{S=0}^{\infty} n_F(\xi_{0N}) |J_{N+S,N}(\boldsymbol{q}_\parallel)|^2 \{\delta[\omega - (\Omega_{K0} + S\omega_c)] \right.$$
$$- \delta[\omega + (\Omega_{K0} + S\omega_c)]\} + \sum_{S=1}^{\infty} n_F(\xi_{0N+S}) |J_{N+S,N}(\boldsymbol{q}_\parallel)|^2$$
$$\left. \times \{\delta[\omega - (\Omega_{K0} - S\omega_c)] - \delta[\omega + (\Omega_{K0} - S\omega_c)]\} \right). \tag{42}$$

Analogous to the case of the intrasubband modes, the coupled intersubband magnetoplasmon–phonons can only be damped at the particular frequencies $\omega =$

$\pm|\Omega_{K0} - S\omega_c|$ and $\omega = \pm(\Omega_{K0} + S\omega_c)$. But at these certain frequencies $\mathrm{Re}\,\chi_K^H(q_\parallel, \omega)$ has poles and therefore the coupled intersubband modes are *not* Landau damped within the RPA for finite perpendicular quantizing magnetic fields.

The long-wave approximation of the polarization function (41) at $T = 0$ K is obtained by expanding $|J_{NN'}(q_\parallel)|^2$. Expanding to $O(q_\parallel^4)$ we found (see appendix):

$$\begin{aligned}\chi_K^H(q_\parallel, \omega) = \frac{n_{2DEG}}{\hbar}\frac{\Omega_{K0}}{(\omega^2 - \Omega_{K0}^2)}\left(2 - n_{2DEG}\pi l_0^4 q_\parallel^2 + n_{2DEG}^2\frac{\pi^2 l_0^8}{4}q_\parallel^4\right)\\ + \frac{n_{2DEG}l_0^2}{2\hbar}q_\parallel^2\left((n_{2DEG}\pi l_0^2 - 1)\frac{\Omega_{K0} - \omega_c}{\omega^2 - (\Omega_{K0} - \omega_c)^2}\right.\\ \left. + (n_{2DEG}\pi l_0^2 + 1)\frac{\Omega_{K0} + \omega_c}{\omega^2 - (\Omega_{K0} + \omega_c)^2}\right)\\ - \frac{n_{2DEG}l_0^4}{12\hbar}q_\parallel^4\left((n_{2DEG}\pi l_0^2 + 1)(2n_{2DEG}\pi l_0^2 + 1)\frac{\Omega_{K0} + \omega_c}{\omega^2 - (\Omega_{K0} + \omega_c)^2}\right.\\ + (n_{2DEG}\pi l_0^2 - 1)(2n_{2DEG}\pi l_0^2 - 1)\frac{\Omega_{K0} - \omega_c}{\omega^2 - (\Omega_{K0} - \omega_c)^2}\\ - \tfrac{1}{2}(n_{2DEG}\pi l_0^2 - 1)(n_{2DEG}\pi l_0^2 - 2)\frac{\Omega_{K0} - 2\omega_c}{\omega^2 - (\Omega_{K0} - 2\omega_c)^2}\\ \left. - \tfrac{1}{2}(n_{2DEG}\pi l_0^2 + 1)(n_{2DEG}\pi l_0^2 + 2)\frac{\Omega_{K0} + 2\omega_c}{\omega^2 - (\Omega_{K0} + 2\omega_c)^2}\right).\end{aligned} \tag{43}$$

Another useful approximation of the polarization function is obtained in the case where only the lowest Landau level is filled. In this case $n_F(\xi_{KN})$ is not zero only for $K = N = 0$ (note that we are working within the electric quantum limit at $T = 0$ K) and one immediately obtains from (41) the full RPA result:

$$\chi_K^H(q_\parallel, \omega) = \frac{2\exp(-l_0^2 q_\parallel^2/2)}{\hbar\pi l_0^2}\sum_{N=0}^{\infty}\frac{1}{N!}\left(\frac{l_0^2 q_\parallel^2}{2}\right)^N\frac{N\omega_c + \Omega_{K0}}{(\omega + i\delta)^2 - (N\omega_c + \Omega_{K0})^2}. \tag{44}$$

By including only the contributions from transitions between the $N = 0$ ($K = 0$) and the $N = 0, 1, 2$ ($K > 0$) Landau levels and expanding the exponential function one again recovers the long-wave approximation (43), but without the terms $\sim(n_{2DEG}\pi l_0^2 - 1)$ due to the fact that only the lowest Landau level is filled.

4. Collective excitations

The dispersion relation of the coupled magnetoplasmon–phonons is given by (28) with the polarization functions of sections 3.2 and 3.3.

Without any coupling to the magnetoplasmons the spectrum of the long-wave optical phonons of the DHS is that of dispersion-free LO phonons $\omega_{L\nu}$ which are confined modes in each individual layer ν, and of the interface phonons. For the single-layer geometry of the DHS there are two types of interface modes (Fuchs and Kliewer 1965):

(i) antisymmetric modes $\omega_{A\pm}(q_\parallel)$, and
(ii) symmetric modes $\omega_{S\pm}(q_\parallel)$.

The symmetry properties of the DHS provide the selection rules that even parity modes only induce transitions of electrons between subbands with equal parity and odd parity modes only induce transitions of electrons between subbands with opposite parity. Notice that the interaction of the electrons confined inside the GaAs layer is zero with the LO phonons of $Ga_{0.75}Al_{0.25}As$, because the electric field associated with this mode is zero inside the GaAs layer and at the interfaces.

For numerical work we have chosen a $Ga_{0.75}Al_{0.25}As$–GaAs–$Ga_{0.75}Al_{0.25}As$ DHS with material constants (Adachi 1985) which are, for GaAs:

$$\varepsilon_{\infty 1} = 10.90,\ \omega_{L1} = 5.496 \times 10^{13}\ s^{-1},\ \omega_{T1} = 5.057 \times 10^{13}\ s^{-1}$$

and for $Ga_{0.75}Al_{0.25}As$

$$\varepsilon_{\infty 2} = 10.22,\ \omega_{L2} = 6.979 \times 10^{13}\ s^{-1},\ \omega_{T2} = 6.731 \times 10^{13}\ s^{-1}.$$

We use $m = 0.06624m_0$ for the conduction band mass of GaAs.

4.1. Coupled intrasubband magnetoplasmon-phonons

At first we discuss the dispersion of the coupled intrasubband magnetoplasmon–phonons using the long-wave approximation (37) of the polarization function and retaining only the term $O(q_\parallel^2)$. Within this approximation the dispersion relation (28) decribes the coupled (principal) magnetoplasmon–phonons. Higher roots, describing the Bernstein modes, do not occur. In figure 2 we have plotted the dispersion relations for three different values of the magnetic field. Due to the symmetry properties of the DHS the intrasubband magnetoplasmon ω_{mp}^{00} couples only to the LO phonons ω_{L1} of the GaAs layer and to the symmetric interface phonons $\omega_{S\pm}$, but not to the antisymmetric one. The dispersion curve of the intrasubband magnetoplasmon ω_{mp}^{00} starts for $q_\parallel = 0$ at $\omega = \omega_c$. That means the magnetic field increases the electronic resonance frequency from $\omega = 0$ for $B = 0$ to $\omega = \omega_c$ for $B \neq 0$. If the cyclotron frequency ω_c lies below (figure 2(*a*)) or between (figure 2(*b*)) the dispersion curves of the long-wave optical phonons, the dispersion curve of the intrasubband magnetoplasmon crosses these dispersion curves. Hence, resonance-split dispersion curves of the strongly coupled intrasubband magnetoplasmon–phonon modes occur. In the case that ω_c is larger than the optical phonon frequencies (figure 2(*c*)), the magnetoplasmon–phonon coupling is weak.

The dispersion relation (28) with the long-wave form $\chi_0^H(\boldsymbol{q}_\parallel, \omega) \sim O(q_\parallel^2)$ contains many special cases. The coupled excitation: strict 2D magnetoplasmon–3D LO phonon of the semiconductor $\nu = 1$ (Tselis and Quinn 1984b) is found from (28) by use of $|\varphi(z)|^2 = \delta(z)$ in (22) and retaining only the contribution of 3D LO phonons to $V_{00}^{ph}(\boldsymbol{q}_\parallel, \omega)$, which is given by equation (34) if one replaces $\varepsilon_{\infty 2}$, ε_{s2} and ω_{L2} by $\varepsilon_{\infty 1}$, ε_{s1} and ω_{L1}, respectively. In this case the dispersion relation is:

$$\omega_\pm = [\tfrac{1}{2}\{(\omega_{L1}^2 + \omega_{mp}^2) \pm [(\omega_{L1}^2 - \omega_{mp}^2)^2 + 4(\omega_{L1}^2 - \omega_{T1}^2)(\omega_{mp}^2 - \omega_c^2)]^{1/2}\}]^{1/2}. \tag{45}$$

In equation (45) ω_{L1} and ω_{T1} are the longitudinal and transverse (LO and TO) phonon frequencies and $\varepsilon_{\infty 1}$ and ε_{s1} are the optical and the static dielectric constant of the semiconductor material forming the layer of the DHS. The dispersion relation of the 2D magnetoplasmons (Chaplik 1972) is given by

$$\omega_{mp} = (\omega_p^2 + \omega_c^2)^{1/2} \tag{46}$$

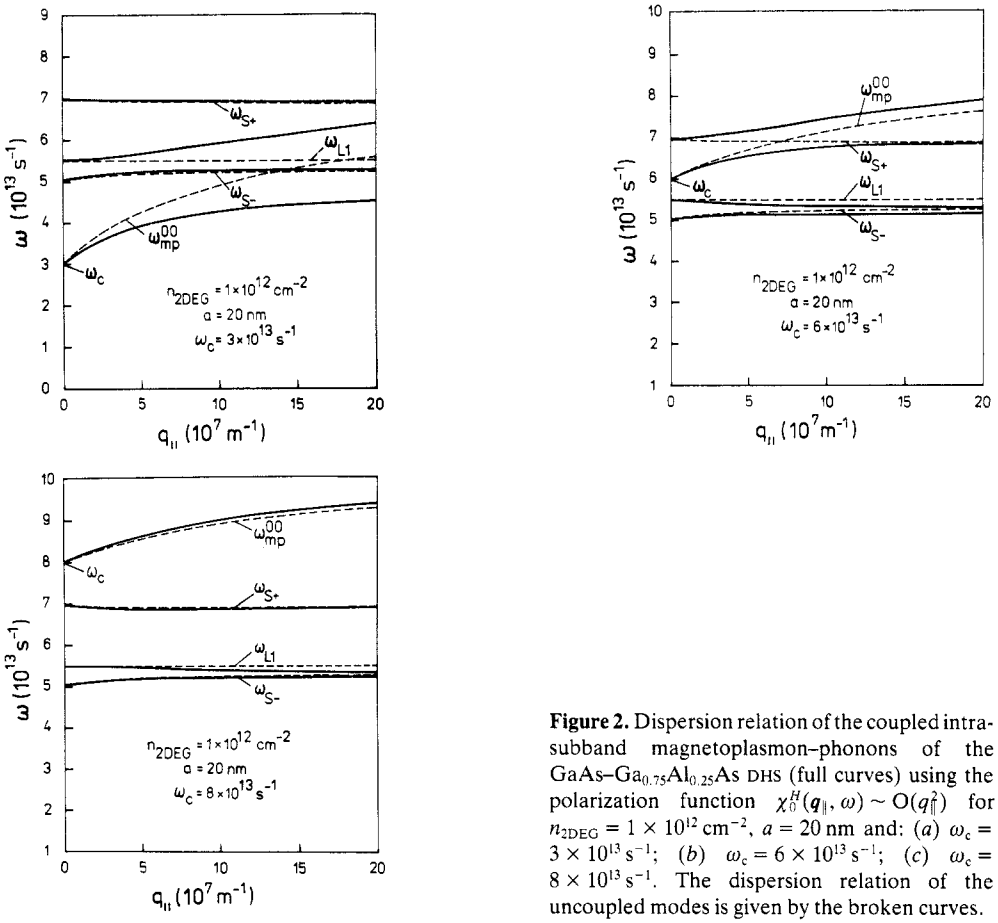

Figure 2. Dispersion relation of the coupled intra-subband magnetoplasmon–phonons of the GaAs–$Ga_{0.75}Al_{0.25}As$ DHS (full curves) using the polarization function $\chi_0^H(\boldsymbol{q}_\parallel, \omega) \sim O(q_\parallel^2)$ for $n_{2DEG} = 1 \times 10^{12}\,cm^{-2}$, $a = 20$ nm and: (*a*) $\omega_c = 3 \times 10^{13}\,s^{-1}$; (*b*) $\omega_c = 6 \times 10^{13}\,s^{-1}$; (*c*) $\omega_c = 8 \times 10^{13}\,s^{-1}$. The dispersion relation of the uncoupled modes is given by the broken curves.

and

$$\omega_p = [(n_{2DEG}e^2/2m\varepsilon_0\varepsilon_{\infty 1})q_\parallel]^{1/2} \tag{47}$$

is the 2D plasma frequency. For a Q2DEG in the presence of a perpendicular magnetic field the dispersion relation of Q2D magnetoplasmons is found from (28) by neglecting the contribution from the phonons $V_{00}^{ph}(\boldsymbol{q}_\parallel, \omega) = 0$ to be:

$$\omega_{mp}^{00} = [(\omega_p^{00})^2 + \omega_c^2]^{1/2} \tag{48}$$

with

$$\omega_p^{00} = [(n_{2DEG}e^2 q_\parallel/2m\varepsilon_0\varepsilon_{\infty 1})f_{00}^c(\boldsymbol{q}_\parallel)]^{1/2}. \tag{49}$$

In equation (49) $f_{00}^c(\boldsymbol{q}_\parallel)$ is the form factor of the Coulomb interaction, which is given by the double integral in (22) for $K_1 = K_2 = K_3 = K_4 = 0$. The corresponding dispersion relation ω_+ of the strict 2D magnetoplasmon–3D LO phonon, which is derived using the full RPA expression of the polarization function (39) including only the transition from the Landau level $N = 0$ to $N = 1$, follows from (28) and (39) (Oji and MacDonald 1986b). It is found that the result is identical with (45) but herein

$$\omega_{mp} = \{\omega_c^2 + \omega_c(e^2 q_\parallel/2\varepsilon_0\varepsilon_{\infty 1}\hbar\pi)\exp[-(l_0^2/2)q_\parallel^2]\}^{1/2} \tag{50}$$

is the RPA magnetoplasmon frequency. It can be seen that these special cases, which are

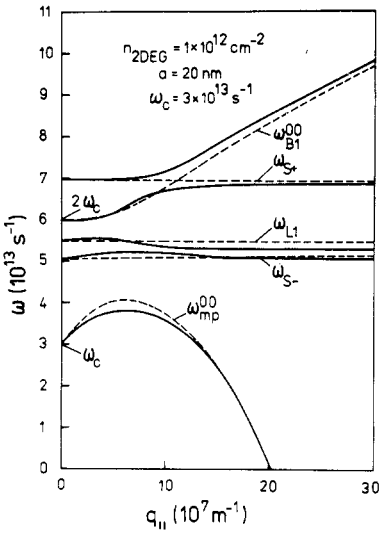

Figure 3. Dispersion relation of the coupled intrasubband magnetoplasmon–phonons of the GaAs–$Ga_{0.75}Al_{0.25}As$ DHS (full curves) using the polarization function $\chi_1^H(q_\parallel, \omega) \sim O(q_\parallel^4)$ for $n_{2DEG} = 1 \times 10^{12}\,cm^{-2}$, $a = 20\,nm$ and $\omega_c = 3 \times 10^{13}\,s^{-1}$. The dispersion relation of the uncoupled modes is given by the broken curves.

obtained from our dispersion relation (28), are connected with the loss of important modes for the case of the DHS. But these simplifying assumptions are mostly used in the literature in order to get a closed analytical result.

The next step of the investigation is to consider the dispersion relation (28) with the full long-wave form of the polarization function given in equation (37). In this case the dispersion relation also describes the lowest-order Bernstein mode. In figure 3 we have plotted the corresponding dispersion curves of the magnetoplasmon–phonons. The principal intrasubband magnetoplasmon mode starts for $q_\parallel = 0$ at $\omega = \omega_c$ whereas the lowest-order intrasubband Bernstein mode starts at $\omega = 2\omega_c$. The principal mode couples to the Bernstein mode as well as to the symmetric optical phonon modes. It can be seen that the dispersion curve of the Bernstein mode ω^{00}_{B1} is resonantly split with the higher frequency symmetric interface phonon mode ω_{S+} for the chosen value of the parameters. The dispersion curve of the intrasubband magnetoplasmon vanishes at $q_\parallel \approx 20 \times 10^7\,m^{-1}$. The collapse of the mode for large wavevectors is originated by the long-wave approximation of the polarization function used in the calculation and not by any physical reason. This can be seen by considering the RPA expression (39) of the polarization function. Expanding the exponential function in a power series, this series consists of terms with alternating signs. Hence, if one were to include all terms in this series and then calculate the dispersion curves, this collapse would not occur. Nevertheless, in most experimental situations the possible wavevector region is restricted to $q_\parallel \lesssim 5 \times 10^7\,m^{-1}$ and, therefore, the long-wave approximation used gives appropriate results.

In figure 4 we have plotted the dispersion curves equivalent to figure 3 but dependent on the magnetic field. For low values of the magnetic field all modes are almost uncoupled. At $B \approx 4\,T$ a strong interaction between the principal magnetoplasmon ω^{00}_{mp} and the Bernstein mode ω^{00}_{B1} takes place, resulting in resonant splitting. For higher magnetic fields (B = 10–14 T) the dispersion curve of the Bernstein mode and that of the principal magnetoplasmon (B = 18–25 T) cross the dispersion curves of the optical phonons. It can be seen that the coupling with phonons is stronger for the principal mode than for the Bernstein mode.

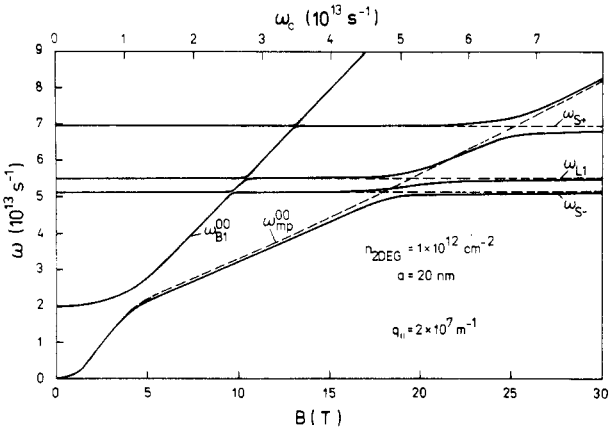

Figure 4. Dispersion relation of the coupled intrasubband magnetoplasmon–phonons of the GaAs–$Ga_{0.75}Al_{0.25}As$ DHS (full curves) using the polarization function $\chi_0^H(\boldsymbol{q}_\parallel, \omega) \sim O(q_\parallel^4)$ for $n_{2DEG} = 1 \times 10^{12}\,cm^{-2}$, $a = 20\,nm$ and $q_\parallel = 2 \times 10^7\,m^{-1}$. The dispersion relation of the uncoupled modes is given by the broken curves.

The interaction of the principal mode with the first Bernstein mode was experimentally investigated by Batke *et al* (1985) with far infrared transmission spectroscopy on GaAs–$Ga_{1-x}Al_xAs$ heterostructures. The results obtained here agree qualitatively very well with the experiment. It was found that the strength of this non-local interaction is given by the parameter $(q_\parallel v_F/\omega_c)^2$. It is possible to rearrange the polarization function (37) to give the dependence on the parameter $(q_\parallel v_F/\omega_c)^2$:

$$\chi_0^H(\boldsymbol{q}_\parallel, \omega) = \frac{m}{2\pi\hbar^2}\left[\left(\frac{q_\parallel v_F}{\omega_c}\right)^2 \frac{\omega_c^2}{\omega^2 - \omega_c^2} - \left(\frac{q_\parallel v_F}{\omega_c}\right)^4 \left(\frac{\omega_c^2}{\omega^2 - \omega_c^2} - \frac{\omega_c^2}{\omega^2 - (2\omega_c)^2}\right)\right]. \tag{51}$$

The result obtained here for the interaction between both modes also corresponds to that of Chaplik and Heitmann (1985), who calculated the absorption of an electric field by strict 2D magnetoplasmons using the classical kinetic theory.

The dispersion relation (28) with the full long-wave form of the polarization function (37) contains many special cases. If we neglect the contribution from the long-wave optical phonons by setting $V_{00}^{ph}(\boldsymbol{q}_\parallel, \omega) = 0$ the dispersion relation of Q2D magnetoplasmons follows:

$$\omega_{mp\pm}^{00} = \left(\tfrac{1}{2}\left[\left[5\omega_c^2 + (\omega_p^{00})^2\right] \pm \left\{\left[3\omega_c^2 - (\omega_p^{00})^2\right]^2 + 6n_{2DEG}\pi l_0^4 q_\parallel^2 (\omega_p^{00}\omega_c)^2\right\}^{1/2}\right]\right)^{1/2}. \tag{52}$$

The (−) mode is the principal intrasubband magnetoplasmon ω_{mp}^{00} (also called in gas plasma physics an upper hybrid mode) and the (+) mode is the intrasubband Bernstein mode ω_{B1}^{00}. Both modes are coupled. The principal magnetoplasmon $\omega_{mp}^{00} = [(\omega_p^{00})^2 + \omega_c^2]^{1/2}$ is degenerated with the higher resonance at $\omega = 2\omega_c$ yielding:

$$q_\parallel^* = 6m\varepsilon_0\varepsilon_{\infty 1}\omega_c^2/n_{2DEG}e^2 f_{00}^c(\boldsymbol{q}_\parallel^*). \tag{53}$$

For values $q_\parallel \ll q_\parallel^*$ the dispersion relation (52) falls into two separate parts. For the principal magnetoplasmon:

$$\omega_{mp-}^{00} = \left((\omega_{mp}^{00})^2 + \frac{\frac{3}{2}n_{2DEG}\pi l_0^4 q_\parallel^2 (\omega_p^{00}\omega_c)^2}{(\omega_{mp}^{00})^2 - (2\omega_c)^2}\right)^{1/2} \tag{54}$$

where the last term in the root of (52) is a non-local correction to the mode ω_{mp}^{00}. The

Bernstein mode dispersion is given in this case by:

$$\omega_{\mathrm{mp}+}^{00} = \left((2\omega_c)^2 - \frac{\frac{3}{2} n_{2\mathrm{DEG}} \pi l_0^4 q_\parallel^2 (\omega_p^{00} \omega_c)^2}{(\omega_{\mathrm{mp}}^{00})^2 - (2\omega_c)^2} \right)^{1/2} . \tag{55}$$

The corresponding relations in the strict 2D case follow from (52) to (55) replacing only $\omega_{\mathrm{mp}}^{00}$, ω_p^{00} and f_{00}^c by ω_{mp}, ω_p and 1, respectively. The equations (54) and (55) give good results also for the real system if $q_\parallel < q_\parallel^*$ and the frequencies of the magnetoplasmon modes are very different from those of the optical phonons. Because $q_\parallel \ll q_\parallel^*$ means very small values of the wavevector or large values of the magnetic field, it is important to know the validity of the equations (54) and (55) in comparison to the frequencies of the optical phonons. If the dispersion curves are well described by (54) and (55) above the dispersion curves of the optical phonons, then the corresponding dielectric constant of the background is $\varepsilon_{\infty 1}$. But in the other case, if the dispersion curves are well described by (54) and (55) far below the dispersion curves of the optical phonons, the corresponding dielectric constant of the background is ε_{s1}, the static dielectric constant. If one replaces $\varepsilon_{\infty 1}$ by ε_{s1} in (54) and (55) the contribution of the optical phonons is included by the ε_s approximation.

4.2. Coupled intersubband magnetoplasmon–phonons

In this subsection we discuss the (1–0) coupled intersubband magnetoplasmon–phonons. As in the case of the intrasubband modes we want to start our analysis using the long-wave approximation (43) of the polarization function for which we retain only the terms $\sim O(q_\parallel^2)$. Within this approximation the dispersion relation (28) describes the coupled principal magnetoplasmon–phonons as well as the first Bernstein mode. In figure 5 we have plotted the dispersion relation for three different values of the magnetic field.

Due to the symmetry properties of the DHS the (1–0) intersubband magnetoplasmons—both the principal mode $\omega_{\mathrm{mp}}^{10}$ and the Bernstein modes $\omega_{\mathrm{B1}\pm}^{10}$—couple only to the LO phonons ω_{L1} of the GaAs layer and to the antisymmetric interface phonons $\omega_{\mathrm{A}\pm}$, but not to the symmetric one. There are three magnetoplasmon modes $\omega_{\mathrm{mp}}^{10}$, $\omega_{\mathrm{B1}+}^{10}$ and $\omega_{\mathrm{B1}-}^{10}$. The principal mode $\omega_{\mathrm{mp}}^{10}$ starts for $q_\parallel = 0$ at a frequency above the subband separation frequency Ω_{10}, because of the depolarization shift. This is due to the resonance screening. But the first Bernstein modes start for $q_\parallel = 0$ at $\omega_{\mathrm{B1}\pm}^{10} = |\Omega_{10} \pm \omega_c|$ (see equation (67) later). Following this, the Bernstein modes are not shifted by depolarization effects. The dispersion curve of the intersubband principal magnetoplasmon modes depends only weakly on the strength of the magnetic field, whereas the dependence is strong for the intersubband Bernstein modes. This can be seen by comparing figures 5(*a*) to (*c*). For the three chosen values of the magnetic field only the principal mode $\omega_{\mathrm{mp}}^{10}$ crosses the dispersion curves of the optical phonon modes, yielding resonance-split dispersion curves (figure 5(*a*)). The fact that the dispersion curve at $\omega_c = 3 \times 10^{13}\ \mathrm{s}^{-1}$ forms a closed loop and at higher magnetic fields shows a 'reasonable' behaviour is due to the approximation used for the polarization function $\chi_1^H(q_\parallel, \omega)$ in calculating the dispersion relation. Because the long-wave approximation (43) is essentially a power series expansion in the parameter $(q_\parallel l_0)^2 \sim q_\parallel^2/B$, the dispersion curves at low magnetic fields are correct only at low wavevectors. In the case of $\omega_c = 3 \times 10^{13}\ \mathrm{s}^{-1}$ and for a wavevector of $q_\parallel = 2 \times 10^7\ \mathrm{m}^{-1}$, realizable in experiments, the parameter is $(q_\parallel l_0)^2 = 0.024$ and for $q_\parallel = 5 \times 10^7\ \mathrm{m}^{-1}$ this parameter is 0.15. Hence, in the small wavevector region ($q_\parallel \lesssim 5 \times 10^7\ \mathrm{m}^{-1}$) the calculated dispersion curves of figures 5(*a*)–(*c*) are of sufficient accuracy.

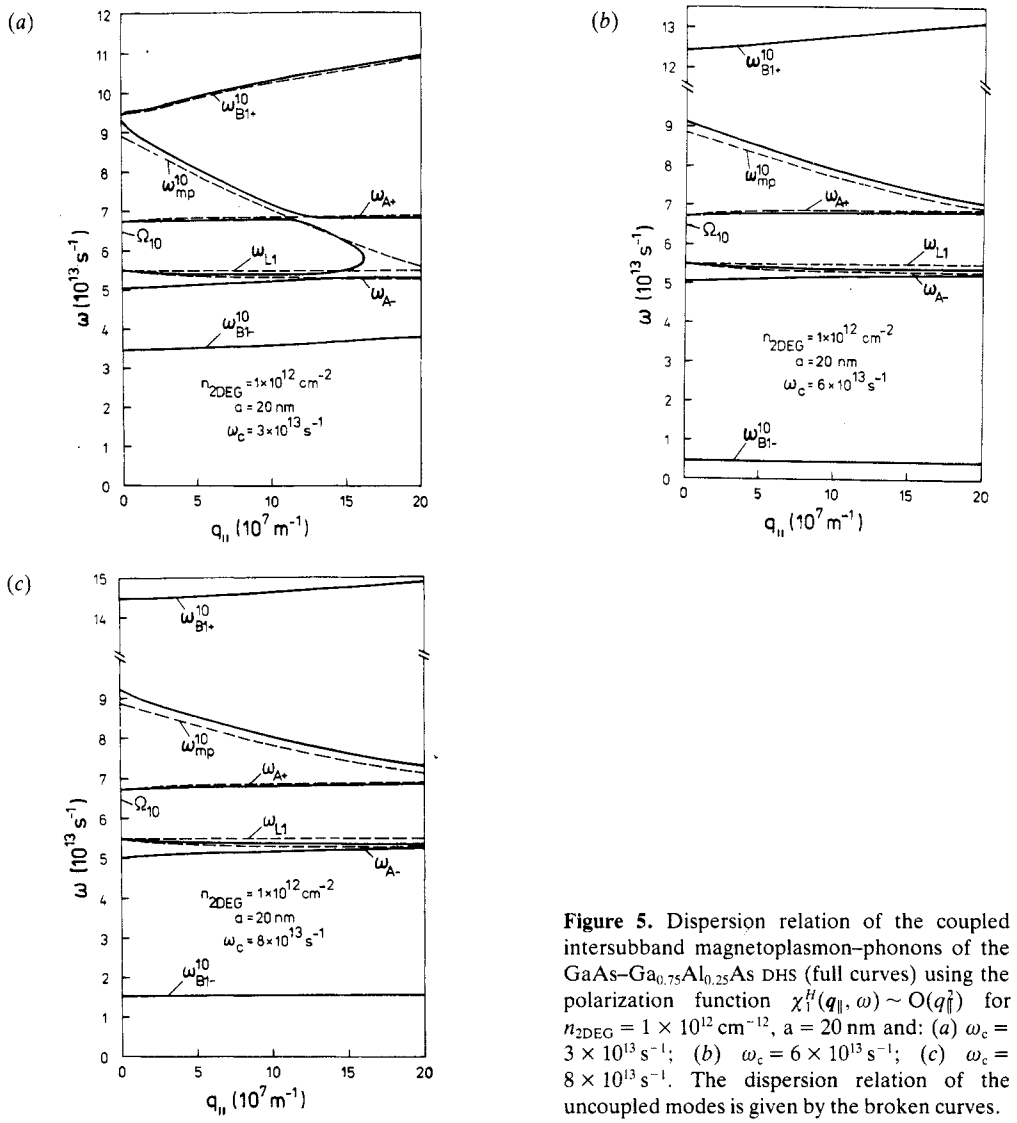

Figure 5. Dispersion relation of the coupled intersubband magnetoplasmon–phonons of the GaAs–$Ga_{0.75}Al_{0.25}As$ DHS (full curves) using the polarization function $\chi^H_\uparrow(\boldsymbol{q}_\parallel, \omega) \sim O(q^2_\parallel)$ for $n_{2DEG} = 1 \times 10^{12}\,cm^{-12}$, a = 20 nm and: (*a*) $\omega_c = 3 \times 10^{13}\,s^{-1}$; (*b*) $\omega_c = 6 \times 10^{13}\,s^{-1}$; (*c*) $\omega_c = 8 \times 10^{13}\,s^{-1}$. The dispersion relation of the uncoupled modes is given by the broken curves.

If we expand $V^\infty_{11}(\boldsymbol{q}_\parallel)$ (equation (22)) in a power series of $q_\parallel$ according to:

$$V^\infty_{11}(\boldsymbol{q}_\parallel) = \frac{\hbar\Omega_{10}}{2n_{2DEG}}(\alpha_{11} - \mu_{11}q_\parallel - \gamma_{11}q^2_\parallel) + O(q^3_\parallel) \tag{56}$$

with

$$\alpha_{11} = \frac{n_{2DEG}}{\hbar\Omega_{10}}\frac{e^2}{\varepsilon_0\varepsilon_{\infty 1}}\frac{10a}{9\pi^2} \tag{57}$$

$$\mu_{11} = \frac{n_{2DEG}}{\hbar\Omega_{10}}\frac{e^2}{\varepsilon_0\varepsilon_{\infty 1}}\frac{256a^2}{81\pi^4} \tag{58}$$

$$\gamma_{11} = -\frac{n_{2DEG}}{\hbar\Omega_{10}}\frac{e^2}{\varepsilon_0\varepsilon_{\infty 1}}\frac{46a^3}{81\pi^4} \tag{59}$$

we can derive an explicit dispersion relation for the (1–0) intersubband magnetoplasmon in the absence of optical phonons. Using $\chi_1^H(\boldsymbol{q}_\parallel, \omega) \sim O(q_\parallel)$ and $V_{11}^\infty(\boldsymbol{q}_\parallel) \sim O(q_\parallel)$ in the dispersion relation (28) with $V_{11}^{ph}(\boldsymbol{q}_\parallel, \omega) = 0$ the dispersion relation (28) reads:

$$\omega_{mp}^{10} = [(1 + \alpha_{11})\Omega_{10}^2 - \mu_{11}\Omega_{10}^2 q_\parallel + O(q_\parallel^2)]^{1/2}. \tag{60}$$

This is the same result as in the case with no magnetic field (see for instance equation (65) of Wendler and Pechstedt 1987b). It is important to note that the magnetic field only affects the terms higher than $O(q_\parallel)$. This explains the weak dependence of the principal intersubband magnetoplasmon on the magnetic field. Within this approximation ($\chi_1^H \sim O(q_\parallel)$, $V_{11}^\infty \sim O(q_\parallel)$) it is also possible to calculate the dispersion relation of the coupled excitations for the special case of the principal intersubband magnetoplasmon–3D LO phonon coupling in explicit form. Using the vertex function $M_{10}^{LO}(\boldsymbol{q}_\parallel)$ of the 3D LO phonons one immediately obtains from (21) and (56):

$$V_{11}^{ph}(\boldsymbol{q}_\parallel, \omega) = \frac{\hbar\Omega_{10}}{2n_{2DEG}}(\alpha_{11} - \mu_{11}q_\parallel)\frac{\omega_{L1}^2 - \omega_{T1}^2}{\omega^2 - \omega_{L1}^2} + O(q_\parallel^2). \tag{61}$$

Using this in (28) we find

$$\omega_\pm = [\tfrac{1}{2}[\omega_{L1}^2 + \Omega_{10}^2(1 + \alpha_{11} - \mu_{11}q_\parallel)] \pm \tfrac{1}{2}\{[\omega_{L1}^2 + \Omega_{10}^2(1 + \alpha_{11} - \mu_{11}q_\parallel)]^2 - 4[\omega_{L1}^2 + \omega_{T1}^2(\alpha_{11} - \mu_{11}q_\parallel)]\,\Omega_{10}^2\}^{1/2}]^{1/2}. \tag{62}$$

This very restrictive approximation (3D LO phonons), in comparison to the treatment used here, is most commonly used, if dynamical phonon effects on the intersubband magnetoplasmons are investigated (Tselis and Quinn 1984b).

The next term in the long-wave approximation of the explicit dispersion curve of the (1–0) intersubband magnetoplasmons is found if we use (56) and $\chi_1^H(\boldsymbol{q}_\parallel, \omega) \sim O(q_\parallel^2)$ in (28) for $V_{11}^{ph}(\boldsymbol{q}_\parallel, \omega) = 0$. Using this approximation we found, for the dispersion curves of the (1–0) principal intersubband magnetoplasmon and for the first (1–0) Bernstein modes, the following explicit dispersion relations:

$$\begin{aligned}\omega_{mp}^{10} = [&(1 + \alpha_{11})\Omega_{10}^2 - \mu_{11}\Omega_{10}^2 q_\parallel - \Omega_{10}^2(\gamma_{11} + \tfrac{1}{2}\alpha_{11}n_{2DEG}\pi l_0^4)q_\parallel^2 \\ &+ \tfrac{1}{4}\Omega_{10}^3\alpha_{11}^2 l_0^2 q_\parallel^2(n_{2DEG}\pi l_0^2 - 1)(\omega_c - \Omega_{10})/(\omega_c^2 - 2\omega_c\Omega_{10} - \alpha_{11}\Omega_{10}^2) \\ &- \tfrac{1}{4}\Omega_{10}^3\alpha_{11}^2 l_0^2 q_\parallel^2(n_{2DEG}\pi l_0^2 + 1)(\omega_c + \Omega_{10})/(\omega_c^2 + 2\omega_c\Omega_{10} - \alpha_{11}\Omega_{10}^2)]^{1/2}\end{aligned} \tag{63}$$

$$\omega_{B1+}^{10} = \left((\omega_c + \Omega_{10})^2 + q_\parallel^2/4\,\frac{\Omega_{10}\alpha_{11}l_0^2(n_{2DEG}\pi l_0^2 + 1)(\omega_c + \Omega_{10})(\omega_c + 2\Omega_{10})\omega_c}{\omega_c(\omega_c + 2\Omega_{10}) - \alpha_{11}\Omega_{10}^2}\right)^{1/2} \tag{64}$$

$$\omega_{B1-}^{10} = \left((\omega_c - \Omega_{10})^2 - q_\parallel^2/4\,\frac{\Omega_{10}\alpha_{11}l_0^2(n_{2DEG}\pi l_0^2 - 1)(\omega_c - \Omega_{10})(\omega_c - 2\Omega_{10})\omega_c}{\omega_c(\omega_c - 2\Omega_{10}) - \alpha_{11}\Omega_{10}^2}\right)^{1/2}. \tag{65}$$

From these dispersion curves it is simply possible to obtain the limits:

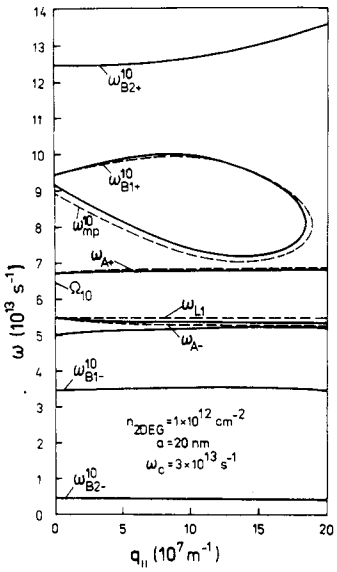

Figure 6. Dispersion relation of the coupled intersubband magnetoplasmon–phonons of the GaAs–$Ga_{0.75}Al_{0.25}As$ DHS (full curves) using the polarization function $\chi_1^H(q_\parallel, \omega) \sim O(q_\parallel^4)$ for $n_{2DEG} = 1 \times 10^{12}\,cm^{-2}$, $a = 20\,nm$ and $\omega_c = 3 \times 10^{13}\,s^{-1}$. The dispersion relation of the uncoupled modes is given by the broken curves.

(i) $q_\parallel \to 0$

$$\omega_{mp}^{10} = (1 + \alpha_{11})^{1/2}\Omega_{10} \tag{66}$$

$$\omega_{B1\pm}^{10} = |\Omega_{10} \pm \omega_c| \tag{67}$$

(ii) $B \to \infty$

$$\omega_{mp}^{10} = [(1 + \alpha_{11})\Omega_{10}^2 - \mu_{11}\Omega_{10}^2 q_\parallel - \gamma_{11}\Omega_{10}^2 q_\parallel^2]^{1/2} \tag{68}$$

$$\omega_{B1\pm}^{10} = \infty. \tag{69}$$

In the next step of the investigation of the (1–0) intersubband modes we consider the dispersion relation (28) with the full long-wave form of the polarization function given in (43). The corresponding dispersion curves are plotted in figure 6.

In this case the spectrum of the (1–0) intersubband magnetoplasmons consists of the principal mode ω_{mp}^{10} and of four Bernstein modes, the first Bernstein modes $\omega_{B1\pm}^{10}$ and the second one, $\omega_{B2\pm}^{10}$. Due to the coupling between these five magnetoplasmons their dispersion curves are altered in comparison to those in figure 5(*a*). In particular, the modes ω_{mp}^{10} and ω_{B1+}^{10} have dispersion curves forming a loop. But it seems that this collapse has no deeper physical reason, since it is caused by the approximate form of the polarization function (43). Because (43) is valid only for small values of the parameter $(q_\parallel l_0)^2$, the dispersion curves are only correct in the region $q_\parallel \lesssim 5 \times 10^7\,m^{-1}$, which is the most interesting one for experiments on magnetoplasmons. From this discussion one can see the important fact that, due to the very rich resonance structure of the spectrum and the strong coupling of the different modes, the theoretical results depend very sensitively on the approximation used. Our calculations show that a sufficiently correct description of the magnetoplasmons demands the use of good approximations for the polarization function. This is a problem because for the full RPA expression of the polarization function it is not possible to calculate an explicit analytic expression.

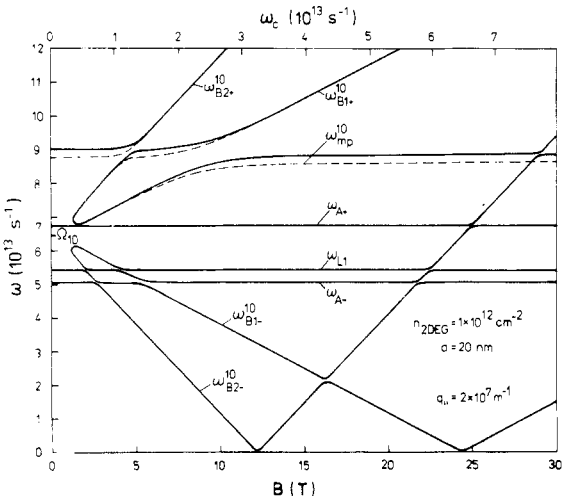

Figure 7. Dispersion relation of the coupled intersubband magnetoplasmon–phonons of the GaAs–$Ga_{0.75}Al_{0.25}As$ DHS (full curves) using the polarization function $\chi^H_1(q_\parallel, \omega) \sim O(q^4_\parallel)$ for $n_{2DEG} = 1 \times 10^{12}\,cm^{-2}$, $a = 20\,nm$ and $q_\parallel = 2 \times 10^7\,s^{-1}$. The dispersion relation of the uncoupled modes is given by the broken curves.

In figure 7 we have plotted the dispersion curves equivalent to those of figure 6 but dependent on the magnetic field. This figure shows the rich resonance structure. It is to be seen that the three modes ω^{10}_{mp}, ω^{10}_{B1+} and ω^{10}_{B2+} lie above the dispersion curves of the optical phonons for all strengths of the magnetic field. The dispersion curves of these modes cross each other at certain magnetic fields yielding the resonance splitting shown. The two lower frequency (1–0) intersubband Bernstein modes cross the dispersion curves ω_{L1} and ω_{A-} at low values of the magnetic field. At higher magnetic fields these modes tend to go to zero frequency. But the dispersion curves ω^{10}_{B1-} and ω^{10}_{B2-} are 'reflected' at $\omega = 0$ because the resonances in (43) are of the form $\omega = |\Omega_{10} - \omega_c|$ and $\omega = |\Omega_{10} - 2\omega_c|$. The result is firstly the crossing of dispersion curves of the magnetoplasmons between each other; and secondly, the crossing of these dispersion curves with those of the optical phonons and of the principal mode ω^{10}_{mp} at higher magnetic fields. Therefore the relatively complicated figure of dispersion curves arises.

To our knowledge, up to now no experimental investigations of the intersubband magnetoplasmons have been made.

5. Concluding remarks

In this paper we have presented a detailed survey of the magnetoplasmons in semiconductor quantum wells, including the effect of electron–phonon coupling. It is shown that the principal intra- and intersubband magnetoplasmons, the intra- and intersubband Bernstein modes, the LO phonons and the interface phonons form a coupled set of modes.

The polarization function of the Q2D magnetoplasmons is calculated in RPA. A detailed discussion of the polarization function shows that Landau damping is impossible for quantizing magnetic fields. Following this, the coupled magnetoplasmon–phonons

are free of Landau damping. This result follows from the unusual ground-state properties of a Q2DEG in a perpendicular quantizing magnetic field. Under such conditions, a completely quantized situation arises for which each energetic level is macroscopically degenerated. Besides the full RPA polarization function we have calculated and discussed different long-wave approximations. In this paper we generalize earlier papers on magnetoplasmons in quantum wells in three ways:

(i) taking into account the finite thickness of the electron system perpendicular to the heterointerfaces;

(ii) including the complete set of long-wavelength optic phonons, i.e. LO and interface phonons;

(iii) using the RPA polarization function of the Q2D magnetoplasma, including the higher resonances.

The effect of the finite thickness of the electron system on the collective excitations is twofold. Firstly the dispersion curve of the intrasubband magnetoplasmon is shifted to lower frequencies and secondly the intersubband magnetoplasmons arise. Following this, neglecting the finite thickness of the electron system, as occurs in most papers, e.g. Chiu and Quinn (1974), MacDonald (1985) and Oji and MacDonald (1986a), only gives good results for the intrasubband modes in the long-wavelength limit. But in this limit ($q_\parallel \approx \sqrt{\varepsilon_{\infty 1}}\,\omega/c$, where c denotes the speed of light in a vacuum) retardation effects will become important (Chiu and Quinn 1974, Wendler and Kändler 1989). We note that all results of this paper are valid in the unretarded limit $q_\parallel \gg \sqrt{\varepsilon_{\infty 1}}\,\omega/c$.

Besides the inclusion of the finite thickness of the electron system, we include for the first time the higher resonances of the magnetoplasma, the Bernstein modes, as well as the LO and the interface phonons. Because of the very complex resonance structure of the magnetoplasmon–phonon system in quantum wells the calculated dispersion curves strongly depend on the approximation of the polarization function used. In this paper we use the RPA. For the case that only one Landau level is filled a closed analytic expression can be derived. Because of the large effects of the size-quantization on the collective modes, its neglect in the work of Horing and Yildiz (1986) is only a good approximation for very large thicknesses of the quantum well ($a \gg \lambda_0$, where λ_0 is the de Broglie wavelength).

Up to now the spectrum of the magnetoplasmon–phonons in quantum wells has not been well investigated experimentally. There exist only experiments on the intrasubband principal magnetoplasmon and its interaction with the first Bernstein mode (Batke *et al* 1985). The intersubband modes as well as the coupling of the modes to the optical phonons of the system is an open field for experiment. Possible problems for experiment are the complex resonance structure and the very low oscillator strength of the higher resonances of the magnetoplasma (Mermin and Canel 1964).

Appendix

In the following we outline the calculation of the polarization function of the quasi-two-dimensional electron gas in the presence of a perpendicular magnetic field. According to equation (18) we have:

$$|J_{N+S,N}(\boldsymbol{q}_\parallel)|^2 = [N!/(N+S)!][(l_0^2/2)q_\parallel^2]^S \exp[-(l_0^2/2)q_\parallel^2]\{L_N^S[(l_0^2/2)q_\parallel^2]\}^2 \qquad S \geqslant 0 \tag{A1}$$

with the associated Laguerre polynomial defined by:

$$L_N^S(\xi) = \frac{e^\xi \xi^{-S}}{N!}\frac{\mathrm{d}^N}{\mathrm{d}\xi^N}(e^{-\xi}\xi^{N+S}) \tag{A2}$$

which gives

$$L_N^S(\xi) = \frac{1}{N!}\sum_{m=0}^{N}\binom{N}{m}(-1)^m\frac{(N+S)!}{(S+m)!}\xi^m. \tag{A3}$$

Using (A3) in (A1) and expanding (A1) in a power series of the parameter $(l_0^2 q_\parallel^2/2)$ gives the following:

$$|J_{N+S,N}(\boldsymbol{q}_\parallel)|^2 = \frac{(N+S)!}{N!(S!)^2}[(l_0^2/2)q_\parallel^2]^S\left[1 - \frac{2N+S+1}{S+1}[(l_0^2/2)q_\parallel^2] + \left(\frac{N^2}{(S+1)^2}\frac{2S+3}{S+2} + \frac{N}{S+1}\frac{2S+3}{S+2} + \frac{1}{2}\right)[(l_0^2/2)q_\parallel^2]^2\right] + \mathrm{O}\{[(l_0^2/2)q_\parallel^2]^{S+3}\}. \tag{A4}$$

For the calculation of the sum of N and S in the polarization function (16) we use the properties of the electric quantum limit for $T = 0$ K

$$n_\mathrm{F}(\xi_{KN}) = \begin{cases} 1 & \text{for } K = 0 \text{ and } N \leqslant \tilde{N} \\ 0 & \text{for } K = 0 \text{ and } N > \tilde{N} \\ 0 & \text{for } K > 0 \end{cases} \tag{A5}$$

where $\tilde{N}$ is the energetic highest Landau level which is occupied. According to the degeneracy of each Landau level (equation (10)) it follows that:

$$\tilde{N} + 1 = \pi n_\mathrm{2DEG}\hbar/m\omega_\mathrm{c}. \tag{A6}$$

Now it is easy to carry out the following sums:

$$\sum_{N=0}^{\infty}|J_{N+1,N}(\boldsymbol{q}_\parallel)|^2\,[n_\mathrm{F}(\xi_{0N}) - n_\mathrm{F}(\xi_{0N+1})] = n_\mathrm{2DEG}\pi l_0^2[(l_0^2/2)q_\parallel^2]\{1 - [(l_0^2/2)q_\parallel^2]\pi n_\mathrm{2DEG}l_0^2\} \tag{A7}$$

$$\sum_{N=0}^{\infty}|J_{N+2,N}(\boldsymbol{q}_\parallel)|^2\,[n_\mathrm{F}(\xi_{0N}) - n_\mathrm{F}(\xi_{0N+2})] = \tfrac{1}{2}(n_\mathrm{2DEG}\pi l_0^2)^2[(l_0^2/2)q_\parallel^2]^2. \tag{A8}$$

These two sums are necessary for the calculation of $\chi_0^H(\boldsymbol{q}_\parallel, \omega)$. To calculate $\chi_K^H(\boldsymbol{q}_\parallel, \omega)$ we use the following sums:

$$\sum_{N=0}^{\infty}n_\mathrm{F}(\xi_{0N})|J_{N,N}(\boldsymbol{q}_\parallel)|^2 = \sum_{N=0}^{\tilde{N}}|J_{N,N}(\boldsymbol{q}_\parallel)|^2 = n_\mathrm{2DEG}\pi l_0^2[1 - n_\mathrm{2DEG}\pi l_0^2(l_0^2q_\parallel^2/2) + \tfrac{1}{2}n_\mathrm{2DEG}^2 l_0^4\pi^2(l_0^2q_\parallel^2/2)^2] \tag{A9}$$

$$\sum_{N=0}^{\infty} n_F(\xi_{0N})|J_{N+1,N}(q_\parallel)|^2 = \sum_{N=0}^{\hat{N}} |J_{N+1,N}(q_\parallel)|^2 = n_{2DEG}\pi l_0^2[\tfrac{1}{2}(n_{2DEG}\pi l_0^2 + 1)$$
$$- \tfrac{1}{6}(n_{2DEG}\pi l_0^2 + 1)(2n_{2DEG}\pi l_0^2 + 1)(l_0^2 q_\parallel^2/2)](l_0^2 q_\parallel^2/2) \tag{A10}$$

$$\sum_{N=0}^{\infty} n_F(\xi_{0N+1})|J_{N+1,N}(q_\parallel)|^2 = \sum_{N=0}^{\hat{N}-1} |J_{N+1,N}(q_\parallel)|^2 = (n_{2DEG}\pi l_0^2 - 1)(l_0^2 q_\parallel^2/2)[n_{2DEG}\pi l_0^2/2$$
$$- n_{2DEG}\pi l_0^2/6 \times (2n_{2DEG}\pi l_0^2 - 1)(l_0^2 q_\parallel^2/2)] \tag{A11}$$

$$\sum_{N=0}^{\infty} n_F(\xi_{0N})|J_{N+2,N}(q_\parallel)|^2 = \sum_{N=0}^{\hat{N}} |J_{N+2,N}(q_\parallel)|^2$$
$$= \tfrac{1}{12} n_{2DEG}\pi l_0^2 (n_{2DEG}\pi l_0^2 + 1)(n_{2DEG}\pi l_0^2 + 2)(l_0^2 q_\parallel^2/2)^2 \tag{A12}$$

$$\sum_{N=0}^{\infty} n_F(\xi_{0N+2})|J_{N+2,N}(q_\parallel)|^2 = \sum_{N=0}^{\hat{N}-2} |J_{N+2,N}(q_\parallel)|^2$$
$$= \tfrac{1}{12} n_{2DEG}\pi l_0^2 (n_{2DEG}\pi l_0^2 - 1)(n_{2DEG}\pi l_0^2 - 2)(l_0^2 q_\parallel^2/2)^2. \tag{A13}$$

With the help of these explicitly given sums it is now easy to calculate equations (37) and (43) from (35) and (41), respectively.

References

Adachi S 1985 *J. Appl. Phys.* **58** R1
Batke E, Heitmann D, Kotthaus J P and Ploog K 1985 *Phys. Rev. Lett.* **54** 2367
Batke E, Heitmann D and Tu C W 1986 *Phys. Rev.* B **34** 6951
Bloss W L and Brody E M 1982 *Solid State Commun.* **43** 523
Bychkov Yu A, Iordanskii S V and Eliashberg G M 1981 *Zh. Eksp. Teor. Fiz., Pisma* **33** 152
Chaplik A V 1972 *Zh. Eksp. Teor. Fiz.* **62** 746
Chaplik A V and Heitmann D 1985 *J. Phys. C: Solid State Phys.* **18** 3357
Chiu K W and Quinn J J 1974 *Phys. Rev.* B **9** 4724
Das Sarma S and Quinn J J 1982 *Phys. Rev.* B **25** 7603
Evans E and Mills D L 1973 *Phys. Rev.* B **8** 4004
Fuchs R and Kliewer K L 1965 *Phys. Rev.* **140** A 2076
Gasser W and Täuber U C 1987 *Z. Phys. B: Condens. Matter* **69** 87
Glasser M L 1983 *Phys. Rev.* B **28** 4387
Horing N J M and Yildiz M M 1976 *Ann. Phys., New York* **97** 216
—— 1986 *Phys. Rev.* B **33** 3895
Kallin C and Halperin B I 1984 *Phys. Rev.* B **30** 5655
Kobayashi M, Mizuno J and Yokota I 1975 *J. Phys. Soc. Japan* **39** 18
Lerner I V and Lozovik Yu E 1978 *Zh. Eksp. Teor. Fiz.* **74** 274
Mahan G D 1972a *Polarons in Ionic Crystals and Polar Semiconductors* ed J T Devreese (Amsterdam: North-Holland) pp 553–657
—— 1972b *Phys. Rev.* B **5** 739
MacDonald A H 1985 *J. Phys. C: Solid State Phys.* **18** 1003
Mermin N D and Canel E 1964 *Ann. Phys., New York* **26** 247
Mohr E G and Heitmann D 1982 *J. Phys. C: Solid State Phys.* **15** L753
Nicholas R J, Haug R J, von Klitzing K and Weimann G 1988 *Phys. Rev.* B **37** 1294
Oji H C A and MacDonald A H 1986a *Phys. Rev.* B **33** 3810
—— 1986b *Phys. Rev.* B **34** 1371
Theis T N, Kotthaus J P and Stiles P J 1977 *Solid State Commun.* **24** 273
Tselis A C and Quinn J J 1984a *Phys. Rev.* B **29** 2021
—— 1984b *Phys. Rev.* B **29** 3318

Wendler L 1985 *Phys. Status Solidi* b **129** 513
—— 1988 *Solid State Commun.* **65** 1197
Wendler L and Grigoryan V G 1989 *Solid State Commun.* **71** 527
Wendler L, Haupt R and Grigoryan V G 1988 *Phys. Status Solidi* b **149** K123
—— 1990 *Physica* B (at press)
Wendler L and Kaganov M I 1986a *Phys. Status Solidi* b **138** K33
—— 1986b *Zh. Eksp. Teor. Phys. Fiz., Pisma* **44** 345 (English Transl.: 1986 *JETP Lett.* **44** 445)
—— 1987 *Phys. Status Solidi* b **142** K63
Wendler L and Kändler E 1990 *Phys. Lett.* A **146** 339
Wendler L and Pechstedt R 1986 *Phys. Status Solidi* b **138** 197
—— 1987a *Phys. Rev.* B **35** 5887
—— 1987b *Phys. Status Solidi* b **141** 129